**Magazine of Civil Engineering. 2019. 85(1). Pp. 15–27**
**Инженерно-строительный журнал. 2019. № 1(85). С. 15–27**

Magazine of Civil Engineering

ISSN 2071-0305

journal homepage: http://engstroy.spbstu.ru/

DOI: 10.18720/MCE.85.2

# Numerical simulation of the turbulent flow over submerged bridge decks

***T.K.C. Thai,***
*University of Transport and Communications, Hanoi, Vietnam*
*E-mail: chittk@utc.edu.vn*

**Keywords:** bridge deck; drag coefficient; flow; turbulence; numerical simulation

**Abstract.** Today climate change is one of the most significant threats and global issues that should be concerned. It causes the increased number of natural disasters such as hurricanes, storms, typhoons and floods. Under these critical hydrological conditions, transportation infrastructure includes bridges easily got submerged, damaged and lead to its failures. Evaluation of bridge stability, hydrodynamic forces acted to bridges and understanding the complex flow behavior in particular during and after flooding plays an important role to estimate the probability of failure risks for existing bridges and optimal design of future bridges. In the present paper, the turbulent flow with high Reynolds number over a fully submerged bridge deck with various length-to-thickness ratios is numerically investigated by using ANSYS FLUENT. The blockage and submergence ratios are defined as 0.23 and 2, respectively. The realizable $k$–$\varepsilon$ model and volume of fraction (VOF) is applied to predict the complex water surface profiles over the bridge deck and turbulence characteristics including backwater effect upstream of the bridge. Effects of the aspect ratio to the drag coefficient are studied.

## *1. Introduction*

Bridge is an essential important infrastructure, a vital joint of the transportation network. Nowadays because of climate change and global warming, number and frequency of natural disasters such as hurricanes, storms, typhoons and floods has increased and caused devastating impacts on transportation infrastructures include bridges. It can cause the inundation, damages and lead to failures of bridge structures which were not designed for critical hydrological conditions.

Vietnam is one of the five countries worst affected by climate change. In Vietnam, there are over 3450 rivers and streams with a 3260 km long coastline. Hence, Vietnam is always at highest risk from natural disaster as recently ranks eighth in the most affected countries by extreme weather events between 1996 and 2015 and fourth among countries with the highest proportion of the population exposed to river flood risk worldwide [1].

According to Ministry of Transportation and Communication, Vietnam's transportation infrastructure was often damaged by the flooding. For example, during October–December 2016 five floods caused heavy damage to the transportation infrastructure, mostly roads and bridges, in the eighteen provinces. Flood flows from upstream rivers inundated the surrounding areas and damaged many bridges. Figure 1(a) shows the picture of A-Sap Bridge partially inundated by the flood. The middle section of this bridge was completely washed away and severed a village with more than 1400 people on November 2, 2016. Figure 2 demonstrates the photo of a collapsed bridge in Binh Dinh Province due to flooding. Four villages of An Nghia and Hoai An communes have been isolated.

Thai, T.K.C. Numerical simulation of the turbulent flow over submerged bridge decks. Magazine of Civil Engineering. 2019. 85(1). Pp. 15–27. DOI: 10.18720/MCE.85.2.

Тхай Т.К.Т. Численное моделирование турбулентных потоков над подтопленными плитами мостов // Инженерно-строительный журнал. 2019. № 1(85). С. 15–27. DOI: 10.18720/MCE.85.2

Table 1 shows the number of damaged and collapsed bridges caused by the floods of 2016 in the four most suffered provinces Binh Dinh, Ninh Thuan, Phu Yen, Quang Ngai, according to the data provided by the provincial governments [2, 3].

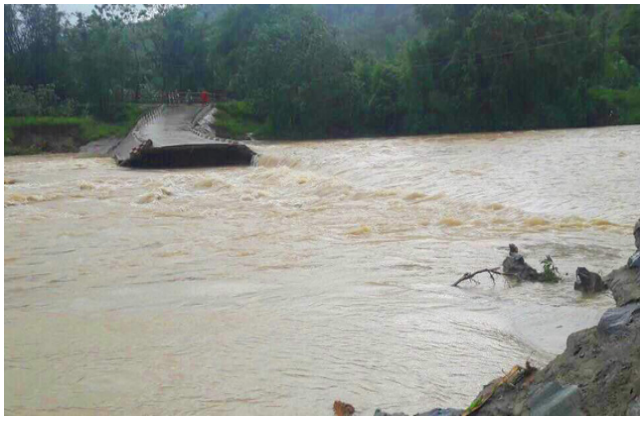

**Figure 1. A-Sap bridge collapsed in Thua Thien Hue province, Vietnam, November 2016.**

**Figure 2. A bridge collapsed in Hoai An, Binh Dinh province, Vietnam, 2016.**

**Table 1. Number of damaged and collapsed bridges.**

| **Province** | Binh Dinh | Ninh Thuan | Phu Yen | Quang Ngai | Total |
|---|---|---|---|---|---|
| **Number of damaged and collapsed bridges** | 57 | 43 | 113 | 40 | 253 |

During flood and other natural disasters, the water level in river rapidly increases and consequently the bridges are got fully or partially submerged. Hydrodynamic forces caused by flood flows strongly affect the bridges structures. It can cause the shearing or overturning of the bridge deck and failure of the bridge superstructures. The bridges subjected to inundated conditions are more liable to failure. Therefore, understanding the complex turbulent flow and determination the hydrodynamic forces acted on the bridge under extreme hydrological conditions are crucial to evaluate the bridge safety, the probability of failure risks for existing bridges and optimal design of future bridges.

In order to estimate the stability of bridges, the drag force plays very important role. The drag force is a combination of viscous (friction) drag and pressure drag (or form drag), which is dependent mainly on the geometry of the body, the location of separation and reattachment points. Generally, the viscous drag on a bridge deck is negligible when compared with the form drag. Some relationships between the drag coefficient and parameters of bridges and flows were examined. Most studies in the literature have studied hydrodynamic forces acting on unsubmerged bridge decks but there are only a few studies about water flow over inundated bridges and the accompanying water surface profiles.

Naudascher and Medlarz (1983) determined theoretically and experimentally the hydrodynamic forces acting on the partially submerged bridge deck. They introduced a relationship between the drag coefficient, the elevation of the bridge and the angle between the flow and the bridge axis. The force coefficients were proposed to estimate the peak hydrodynamic loading acting on the bridge deck induced by flow instability and vortex formation [4].

In 1995, The Federal Highway Administration (FHWA) researched on the hydrodynamic loads on piers and the bridge deck. They suggested a constant value of drag coefficient within the range 2.0 to 2.2 [5]. The drag coefficient for fully or partially submerged bridge superstructure can be calculated using the following equation:

$$F_D = \frac{C_D \rho U_0^2 H}{2}, \quad (1)$$

where $F_D$ is drag force per unit length of bridge, N/m;

$\rho$ is the water density, assumed equal to 1000 kg/m$^3$;

$H$ is depth of submergence, m;

$U_0$ is flow velocity, m/s;

$C_D$ is drag coefficient per unit length.

Okajima A. et. al (1997) analyzed the blockage effect on the drag coefficient for a rectangular bridge deck in a uniform flow at Reynolds number $R_e = 4 \cdot 10^3$. The results showed that drag coefficient depends greatly on blockage ratios $D/H_0$, where $D$ is the thickness of the cylinder and $H_0$ is the depth of the upstream flow [6].

Malavasi & Guadagnini (2003, 2004, 2007) carried out experiments applying a time resolved PIV technique to investigate the flow field and examine the hydrodynamic loading on bridge decks with the aspect ratio of the cylinder was $L/D = 3$ and $L/D = 1$ (where $L$ is the streamwise length of the cylinder) for different submergence levels, Reynolds numbers and deck Froude numbers. Their results showed that due to the presence of a free surface, force coefficients can either be larger (by more than a factor of 2) or lower than the corresponding values of an unbounded domain. The flow fields around the deck had strong asymmetry and a complex vortex-shedding regime. The blockage ratio affects the forces acted on the bridge deck [7–10].

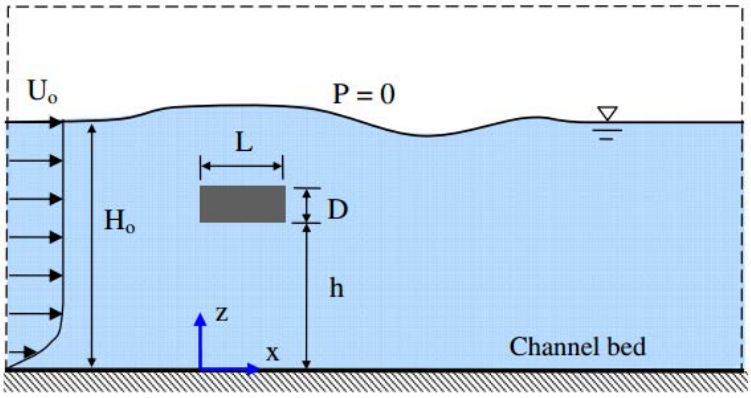


**Figure 3. A Schematic diagram of a fully submerged cylinder (Malavasi & Guadagnini, 2003).**

T. Picek, Havlik, Mattas, & Mares (2007) conducted experiments to calculate of flow through partially and fully submerged rectangular bridge decks of a rectangular shape. They proposed equations for a calculation of the backwater using empirical equations treating the relative height of an obstacle as a major parameter and the discharge of the pressure flow through decks using the scheme dividing the total flow into the pressure flow and the weir flow [11].

In 2008, Malavasi with Trabucchi used a three-dimensional k-ε turbulence model to simulate the hydrodynamic loading and investigate the bounding effects of a solid wall on the flow around a rectangular cylinder with aspect ratio $L/D = 3$ placed in a steady flow, above a solid wall with different gap ratios $h/D$. They found that the pressure distribution in the gap zone highly changes when the cylinder is closed to the wall [12].

Arslan T. et al. (2013) used a large eddy simulation (LES) model and flume experiments to study the flow field around a partially submerged sharp-edged rectangular cylinder. The drag and lift forces were estimated and compared with the measurements. Their results indicated that the drag forces increase with the submergence ratio. The flow separation and reattachment underneath the cylinder and the vortex formation in the wake region were highly affected by the submergence ratio and the turbulence intensity in the approaching flow [13].

Chu C. et al. (2012, 2016) used a Large Eddy Simulation (LES) model to investigate the interactions between a free surface flow and fully submerged bridge decks for different Reynolds number, Froude number, submergence ratio and blockage ratio. He also conducted an experiment in a water flume on a rectangular cylinder with the aspect ratio $L/D = 3$. They concluded that the drag coefficient of the cylinder was dependent on the deck Froude number and blockage ratio, rather than the Reynolds number [14, 15].

In reality most of the bridge decks are quite elongated but all the above mentioned studies only examined the flow over the bridge deck with the aspect ratio $L/D \le 3$. The flow mostly was steady or sub-critical. Results obtained through experiments and numerical simulations mainly by using OpenFOAM. There are no available studies about the water flow over bridge decks with aspect ratios larger than 3. The effect of the free surface mostly was not considered. Besides it, the definition of the drag, lift and moment are clear, but the specific formula is almost impossible based on the theoretical derivation due to the dependence of force coefficients on the shape of objects.

Therefore, the aim of the present paper is to numerically study the behavior of the turbulent flow over the fully submerged bridge deck but with different aspect ratio of the deck $L/D = 1...7$. Based on the obtained data, the relationship between the drag coefficient and the bridge deck's ratio was determined. In order to

reduce the cost and time solving problem, the $2D$ computational domain and boundaries are chosen as economical and reliable approach to provide a valuable view of the flow over submerged bridge decks.

## 2. Methods

In fluid mechanics, the governing equations of fluid flow are the conservation laws of the mass, momentum and energy. According to that, the rate of increase of mass in a fluid element equals the net rate of flow of mass into that fluid element:

$$\frac{\partial \rho}{\partial t}+\frac{\partial(\rho u)}{\partial x}+\frac{\partial(\rho v)}{\partial y}+\frac{\partial(\rho w)}{\partial z}=0, \tag{2}$$

The time rate of change of momentum in a fluid element equals the net rate of momentum flow out of the fluid element plus the sum of forces acting on the fluid element. The momentum equations for incompressible flow called the Navies – Stokes equations have bellowed forms [16, 17]:

$$\rho\frac{Du}{Dt}=\rho g_x-\frac{\partial \rho}{\partial x}+\mu\left(\frac{\partial^2 u}{\partial x^2}+\frac{\partial^2 u}{\partial y^2}+\frac{\partial^2 u}{\partial z^2}\right), \tag{3}$$

$$\rho\frac{Dv}{Dt}=\rho g_y-\frac{\partial \rho}{\partial y}+\mu\left(\frac{\partial^2 v}{\partial x^2}+\frac{\partial^2 v}{\partial y^2}+\frac{\partial^2 v}{\partial z^2}\right), \tag{4}$$

$$\rho\frac{Dw}{Dt}=\rho g_z-\frac{\partial \rho}{\partial z}+\mu\left(\frac{\partial^2 w}{\partial x^2}+\frac{\partial^2 w}{\partial y^2}+\frac{\partial^2 w}{\partial z^2}\right). \tag{5}$$

The increase rate of energy of a fluid particle equals net rate of heat added to the fluid particle plus net rate of work done on the fluid particle. The energy of a fluid is defined as the sum of internal (thermal) energy $\hat{u}$, kinetic energy *k* and gravitational potential energy. In total there are 5 equations (mass, *x*-, *y*-, *z* momentum and energy) with 7 unknowns (density, pressure, velocity, internal energy, temperature).

In this study, numerical simulations were carried out using FLUENT package. This is a strong analysis tool for modeling based on the finite volume method. The finite element method is developed for numerical solution of complex problems in different fields with varying geometries, material types and loadings. In this method, the complex models are first divided into smaller, simpler and solvable elements called finite elements. Then, by assembling the results of solving each element into larger system, the total solution of model is obtained.

Under critical hydrological conditions, the turbulent flow is irregular, random and chaotic flow, characterized by fluctuating velocity. Hence, the most difficulty in numerically modeling the turbulent flow over the bridge deck is the adequate reproduction of the wake region in the downstream and vortex shedding phenomenon. There are different turbulence models available in FLUENT such as Reynolds – Averaged Navier-Stokes (RANS) models, Large Eddy Simulation (LES), Direct Numerical Simulation (DNS) [18, 22–25].

DNS (Direct Numerical Simulation) model requires very small time steps and high cost that is not suitable for practical industrial applications available today. As for the Large Eddy Simulation (LES), the excessively high resolution is required for wall boundary layers that can only be achieved for flows at very low Reynolds number and on very small geometric scales. For this reason in this paper, the realizable $k$-$\varepsilon$ model, one of the RANS models, is chosen to model the turbulent flow over the submerged bridge deck with different aspect ratios.

RANS models are the most economic approach for computing complex turbulent flows. These models simplify the problem to the solution of two additional transport equations and introduce an Eddy-Viscosity (turbulent viscosity) to compute the Reynolds Stresses [19–21, 26–28]. The Reynolds-averaged momentum equations are as follows:

$$\rho\left(\frac{\partial \overline{u_i}}{\partial t}+\overline{u_k}\frac{\partial \overline{u_i}}{\partial x_k}\right)=-\frac{\partial \overline{p}}{\partial x_i}+\frac{\partial}{\partial x_j}\left(\mu\frac{\partial \overline{u_i}}{\partial x_j}\right)+\frac{\partial R_{ij}}{\partial x_j}, \tag{6}$$

Realizable $k$–$\varepsilon$ model was developed by Shih et al. (1994) and contains a different transport equation for the turbulent dissipation rate $\varepsilon$, than the traditional $k$-$\varepsilon$ approach. This turbulence model differs from the other model in two ways: it contains a new alternative formulation for the turbulent viscosity and a new modified transport equation for the $\varepsilon$ derived from an exact equation for the transport of the mean-square vorticity

fluctuations. The term realizable means that the model satisfies some certain mathematical constraints on the Reynolds stresses consistent with the physics of turbulent flows [29–32]

Comparing with standard model, the realizable k-ε model has many advantages such as: more accurately predicts the spreading rate of both planar and round jets; provide superior performance for flows involving rotation, boundary layers under strong adverse pressure gradients, separation, recirculation and strong streamline curvature.

The modeled transport equations for $k$ and $\varepsilon$ in the realizable $k$-$\varepsilon$ model are:

$$\frac{\partial}{\partial t}(\rho k)+\frac{\partial}{\partial x_j}(\rho k u_j)=\frac{\partial}{\partial x_j}\left[\left(\mu+\frac{\mu_t}{\mu_k}\right)\frac{\partial k}{\partial x_j}\right]+G_k+G_b+\rho\varepsilon-Y_M+S_k, \quad (7)$$

$$\frac{\partial}{\partial t}(\rho\varepsilon)+\frac{\partial}{\partial x_j}(\rho\varepsilon u_j)=\frac{\partial}{\partial x_j}\left[\left(\mu+\frac{\mu_t}{\sigma_\varepsilon}\right)\frac{\partial \varepsilon}{\partial x_j}\right]+\rho C_1 S\varepsilon-\rho C_2\frac{\varepsilon^2}{k+\sqrt{\nu\varepsilon}}+C_{1\varepsilon}\frac{\varepsilon}{k}C_{3\varepsilon}G_b+S_\varepsilon, \quad (8)$$

$$C_1=\max\left[0.43,\frac{\eta}{\eta+5}\right], \quad (9)$$

$$\eta=S\frac{k}{\varepsilon}, \quad (10)$$

$$S=\sqrt{2S_{ij}S_{ij}}, \quad (11)$$

where $G_k$ – the generation of turbulence kinetic energy due to the mean velocity gradients;

$G_b$ – the generation of turbulence kinetic energy due to buoyancy;

$Y_M$ – the contribution of the fluctuating dilatation in compressible turbulence to the overall dissipation rate;

$C_2$, $C_{1\varepsilon}$ – constants;

$\sigma_k$, $\sigma_\varepsilon$ – the turbulent Prandtl numbers for $k$ and $\varepsilon$, respectively;

$S_k$, $S_\varepsilon$ – user-defined source terms.

According to Launder et al., the values of the constants in the realizable $k$-$\varepsilon$ model are given in Table 2 [20].

***Table 2. The values of the constants in the realizable k-ε model***

| $C_\mu$ | $C_\mu$ | $C_\mu$ | $\sigma_k$ | $\sigma_\varepsilon$ |
|---|---|---|---|---|
| 0.09 | 1.44 | 1.9 | 1.0 | 1.2 |

Beside the realizable $k$-$\varepsilon$ model, the Volume of Fraction method was considered to determine more accurately the water surface profiles. Based on the obtained data, the drag coefficient can be determined.

The VOF method is proposed by Hirt and Nichols in 1981 [21]. VOF model belongs to the Euler-Euler approach, which is based on the concept of a fractional volume of fluid to calculate the shape and location of a constant-pressure free surface boundary. In this scheme, two or more fluids can be modeled by solving one set of momentum equations for all fluids and for turbulent flows; a single set of turbulence transport equation is solved. The Interface tracking scheme is used to locate free surface flow. It is assumed that two or more fluids in the flow domain are not interpenetrating. The Navier Stoke equations are solved in either Cartesian or cylindrical coordinates.

In this method, the volume fraction α in the two-phase flow varies from 0 to 1 and is obtained from a transport equation:

$$\frac{\partial \alpha}{\partial t}+\frac{\partial}{\partial x_j}(\alpha\bar{u}_j)=0. \quad (12)$$

The value of $\alpha=1$ corresponds to a cell full of water; and $\alpha=0$ to the cell is full of air.

Data from works carried out by Chu (2016) were adopted as benchmark to clarify the accuracy of the FLUENT numerical model in simulating flows over submerged bridge decks. The conditions set for the numerical simulations were the same as those used in the experiment.

Design Modeler and Meshing tool of Workbench were used to create the geometry model and generate the mesh model relatively. The bridge deck is modeled in a rectangular shape. Initial data were: thickness $D = 0.06$ m, distance from the underside of the deck to the channel floor was $h = 0.14$ m, upstream velocity $U = 1$ m/s, water depth of the undisturbed flow $H = 0.26$ m. In this case, the flow is turbulent and supercritical as the Reynolds number equals:

$$\mathrm{Re} = \frac{UD}{\nu} = 60000. \tag{13}$$

The Froude number of the flow and the deck respectively are:

$$Fr = \frac{U}{\sqrt{gH}} = 0.63; \tag{14}$$

$$Fr_D = \frac{U}{\sqrt{gD}} = 1.3. \tag{15}$$

The blockage ratio was defined as:

$$Br = D / H = 0.23. \tag{16}$$

The submergence ratio is the ratio of the depth of water above the bridge deck to its thickness:

$$h^* = (H - h) / D = 2. \tag{17}$$

The size of the computational domain plays a great important role. The upstream and downstream lengths of the computational model are chosen in such way that the inlet and outlet boundary conditions do not significantly influence free surface development, flow around the bridge deck, and forces on the bridge. Because of the turbulent flow, the inlet is placed $30D$ upstream of the deck and the outlet $30D$ downstream to capture the whole velocity field and give accurate results. The same domain is used for all aspect ratios.

The grid near the bridge deck was denser because the flow pattern in the region is more complex and gradually increases away from the bridge deck. The height of first layer near the surface of bridge deck is $0.005D$. The minimum orthogonal quality is larger than 0.6, which is considered as good quality.

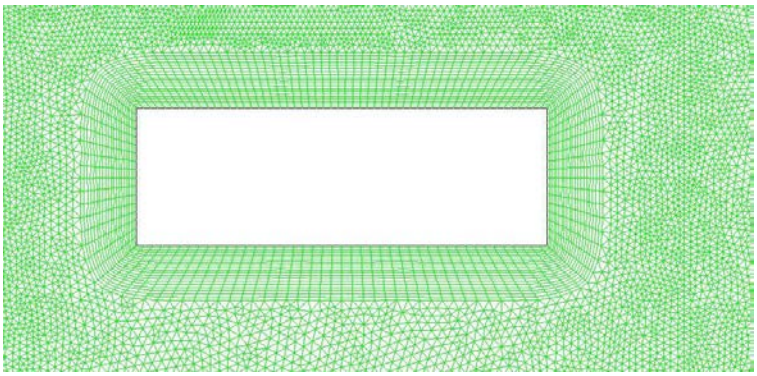

**Figure 4. Mesh in region around bridge deck.**

The boundary conditions for modeling consist of the inlet, the outlet and the walls. Considering the VOF method, the flow domain was divided into two phases, air and water. Air was considered as the secondary phase. The operating pressure is 101325 Pascal. The operating density was set as the density of the lightest phase (air) that is 1.225 kg/m$^3$. Respectively, the inlet has two parts: the lower part where water is coming in and upper part is for air. At the water inlet part, a uniform velocity is applied. The interaction coefficient between water and air is set as 0.072.

The outlet boundary was defined as the pressure outlet used to specify a static gauge pressure at the boundary. Top boundary is given as pressure outlet with a zero atmospheric pressure. Bottom and deck are considered as no-slip wall. The geometry of the $2D$ solution domain and the boundary conditions used for the numerical simulations are shown in Figure 2.

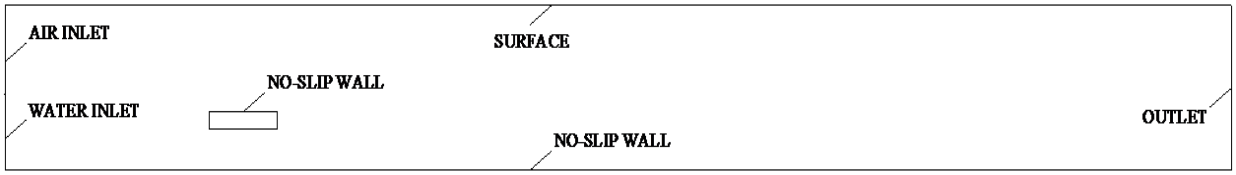


**Figure 5. Computational domain and boundary conditions.**

The numerical solution was considered converged when the residuals of the discretized transport equation reached a value of $1\times10^{-6}$ for all variables including pressure, velocity, turbulent kinetic energy and turbulence dissipation rate. To obtain results more accurately, in the present study, the PISO algorithm (Pressure Implicit with Splitting of Operators) is used for pressure-velocity coupling. The Pressure-Implicit with Splitting of Operators (PISO) pressure-velocity coupling scheme is based on the higher degree of the approximate relation between the corrections for pressure and velocity. The PISO algorithm performs two additional corrections: neighbor correction and skewness correction. It can carry on a stable calculation with larger time step and under-relaxation factors for both momentum and pressure compared to other schemes [18].

Pressure was discretized with a PRESTO Scheme. QUICK Schemes which based on a weighted average of second-order-upwind and central interpolations of the variable is used for pressure discretization and for momentum, kinetic energy and dissipation equations. The inlet flow domain is patched with inlet velocity along with initialization of turbulence kinetic energy and turbulence dissipation rate.

## 3. Results and Discussion

As mentioned in section 2, before employing the numerical model to study the flow over the bridge deck, the numerical simulation for the deck with the aspect ratio $L/D=3$ have been performed and compared with the data from Chu's works in order to validate models using by author. As the results, the drag coefficient, obtained by the present model equals 2.45. Comparing to the drag coefficient obtained by Chu (2016), a good agreement between them has been observed. The error was $(2.64-2.45)\cdot100/2.64=7.2\,\%$.

The simulated water surfaces are compared in Figure 6. Overall, the free surface water profile obtained from the present numerical model shows reasonable agreement with the profile from Chu's model. Based on these mentioned above results, the capability of the present numerical model can be proved.

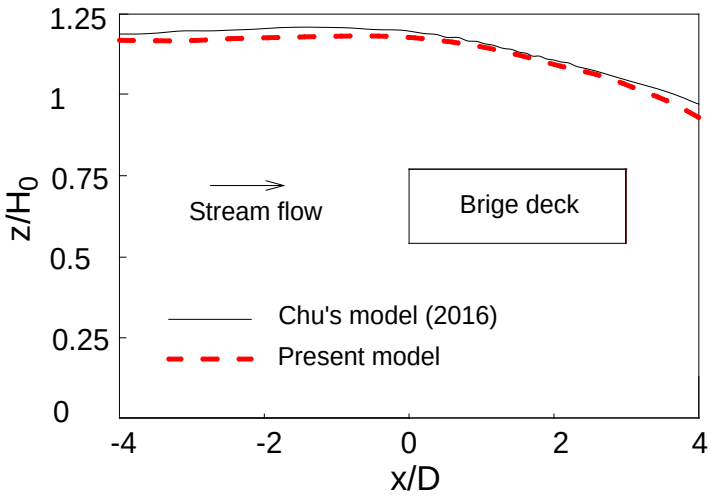


**Figure 6. Free surface water profile of the flow over the decks**

Figure 7 shows the free surface water profiles of the flow over the decks with different aspect ratios $L/D=1;3;5;6$. As the cross-sectional shape of the bridge deck varies, the behavior of the flow changes.

As we can see from these pictures, the shape of water surface profiles over submerged bridge deck is quite complex. First, a backwater effect appeared at the upstream of the deck, the water surface was elevated and then the water surface suddenly dropped and gradually recovered. The deck's aspect ratio decreases, the water level decreased more dramatically at the downstream.

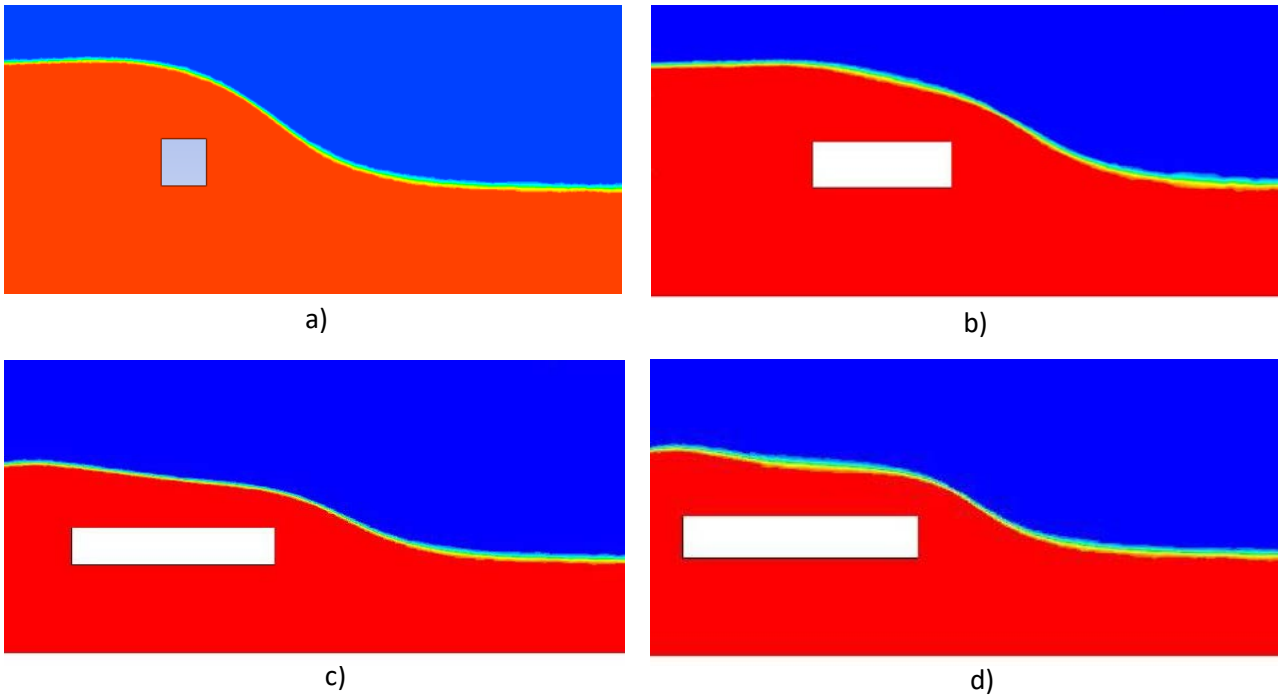


**Figure 7. Free surface water profiles**
**a)** $L/D=1$**; b)** $L/D=3$**; c)** $L/D=5$**; d)** $L/D=6$**.**

The velocity streamlines over the bridge decks are shown in Figure 8. This figure shows that the flow around the decks is significantly affected by the aspect ratios ($L/D$) of the deck. For bridge deck with small aspect ratio $L/D<5$, no reattachment is presented at the lower side due to the short length of the deck. In the case of greater $L/D$ ratio such as $L/D\geq 5$, flow changes from separated to reattachment type of flow. The length of the deck is long enough to allow reattachment of the separated flow. Reattachment of flow along the side surface causes the wake to expand considerably less than the flow without reattachment.

As the shear layer separates at the leading corner, the main vortex is formed along the cylinder side. Under the effect of the free surfaces, vortices around the bridge deck are asymmetry. A small vortex is generated at the upper side of the deck. The reattachment occurs at the end of this vortex.

In case of bridge deck with small aspect ratio $L/D=1$, no vortex is formed right at the bottom of bridge deck. For greater ratios $L/D>1$, a vortex is formed at the lower side with the length about $2D$ in the case $L/D=2$ and then increased to about $3D$. The main vortex acting on the lower side of bridge deck (if existing) always has a longer length than on the upper side.

In the wake region, a reversed flow is generated. Two vortices are formed in the reversed flow region along the rear sides of the deck. The vortices in this reversed flow region fluctuate along the rear sides of the deck. In the case of $L/D=1$, the below vortex placed lower than the bottom side of the deck. As the aspect ratio increases, the place of this vortex is going up and its size also decreases. In the case of $L/D=6$, the two vortices in the wake region are most asymmetry through horizontal middle line of bridge deck. In addition, as the aspect ratio increases, the distance where the shear layers from upper and lower side of the deck meets decreases. For the case of $L/D=1$, this distance is about $2D$ but then decreases to about $1D$ when $L/D=6$.

The drag coefficient of the bridge deck is dependent on the deck aspect ratio. Results of the numerical modeling are presented in Table 3.

The Figure 9 shows the variations of the mean drag coefficient according to the aspect ratio. The largest values of the mean drag coefficient are found for aspect ratio $L/D=2$. As shown in this graph, the drag coefficient is increased quite rapidly as the aspect ratio $L/D$ increased from 1 to 2. But in the case of the aspect ratio $L/D>2$, as the aspect ratio increases, the drag coefficient decreases. In the case of $2<L/D\leq 6$ the difference in drag force between two aspect ratios decreases dramatically but declines slowly when $L/D>6$.

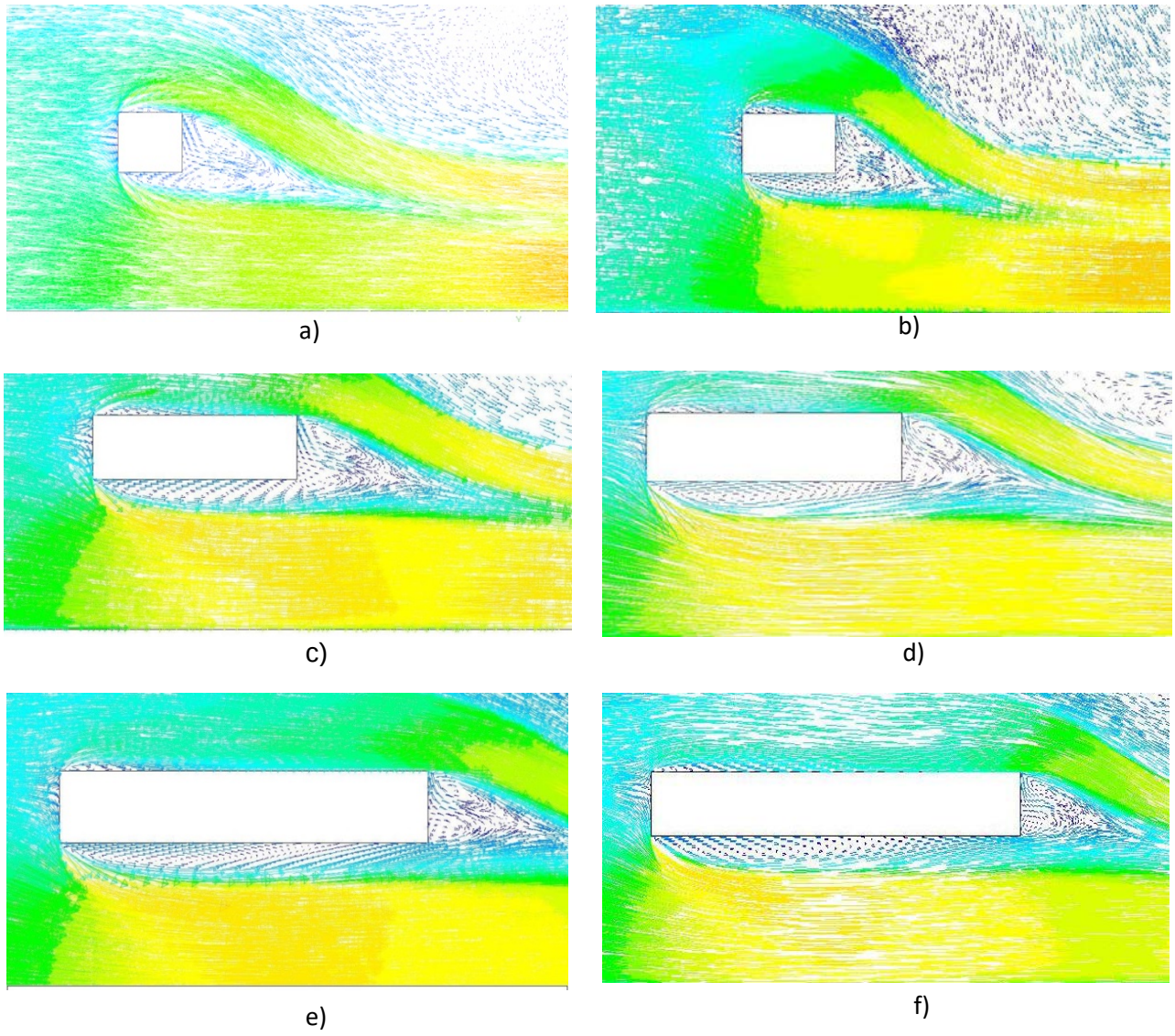


**Figure 8. Structure of flow over bridge deck.**

**a)** $L/D=1$; **b)** $L/D=2$; **c)** $L/D=3$; **d)** $L/D=4$ **e)** $L/D=5$; **f)** $L/D=6$.

***Table 3. Drag coefficient at different aspect ratio of bridge deck.***

| ***L/D*** | 1 | 2 | 3 | 4 | 5 | 6 | 7 |
|---|---|---|---|---|---|---|---|
| $C_D$ | 2.36 | 2.5 | 2.45 | 2.38 | 2.31 | 2.2 | 2.18 |

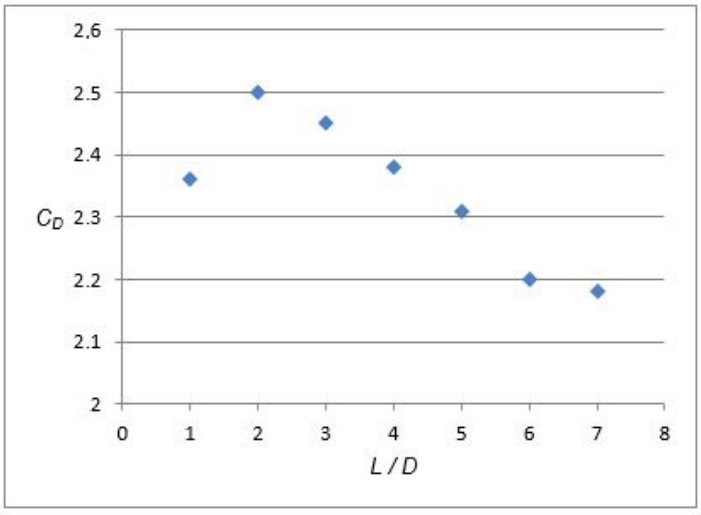


**Figure 9. Variation of the mean drag coefficient according to aspect ratio.**

This tendency can be explained by the fact that the drag force is dependent on the geometry of the bridge deck and the location of separation and reattachment points. From $L/D=1$ to $L/D=2$, the vortex formation region moves closer to the deck and creates the higher base suction. Thus, in this case, the drag force increases. As the aspect ratio increases, the pressure distribution along the side surface of the deck changes, a region of higher pressure called the pressure recovery region occurs after flow reattachment. This pressure recovery region pushes the vortices further downstream. The further downstream the vortices form from the trailing edge of the cylinder, the base suction pressure decreases and also the drag. In another word, as the aspect ratio increases, the effect of the base suction decreases. Besides it, the friction between flows and bridge decks also affects the drag force. As the aspect ratio increases, the frictional effect leads to the increase of the drag force. According to The Federal Highway Administration (FHWA), the submerged bridge deck in these cases is not in safe zone but at high risk of damages as the drag coefficient always larger than 2.1.

## 4. Conclusions

In this study, the numerical modeling was performed for the fully submerged bridge decks with various aspect ratios using ANSYS FLUENT package. The realizable $k$–$\varepsilon$ model and Volume of Fraction method were used to investigate the turbulent flow over the bridge deck.

The present study showed that ANSYS FLUENT software is useful tool to study the turbulent flow without going for expensive and time consuming experiments. The water surface profiles and drag coefficient on submerged bridge decks can be accurately predicted. Effects of the aspect ratio to the flow behavior and drag coefficient are studied. As the aspect ratio of bridge decks decreases, the water level decreased more dramatically at the downstream. The flow changes from separated to reattachment type in the case of $L/D \geq 5$. Two vortices are formed in the reversed flow of the wake region along the rear sides of the deck. As the aspect ratio increases, the distance where the shear layers from upper and lower side of the deck meets also decreases. The largest values of the mean drag coefficient are found for aspect ratio $L/D=2$. In the case of the aspect ratio $L/D>2$, as the aspect ratio increases, the drag coefficient decreases.

The goal of this work is to obtain a better knowledge of the hydrodynamic characteristics of the flow over a bridge deck section with different aspect ratio and determine the drag coefficient in the case of the blockage and submergence ratios were 0.23 and 2, respectively. In future, this work can extend to other cases of different blockage and submergence ratios. Author hopes that it can help researchers to evaluate the bridge safety under critical hydrological conditions.

### References


1. National disaster risk in Vietnam in the period 2006-2016 and forecasting and warning system. National Center for Hydro-Meteological Forecasting. Ministry of Natural Resources and Environment, Vietnam, 2017. 21 p.
2. The World Bank. Vietnam 2016: Rapid Flood Damage and Needs Assessment (RFDNA). 2016. 42 p.
3. NHMS: Statistics of annual major storms (Levels from 6 to 12) struck Vietnam between 1961 and 2014, National Hydro – Meteorological Service (NHMS), Ministry of Natural Resources and Environment, Vietnam, 2015.
4. Naudascher, E., Medlarz, H.J. Hydrodynamic loading and backwater effect of partially submerged bridges. J. Hydraul. Res. 1983. No. 21(3). Pp. 213–232.
5. Federal Highway Administration (FHWA). Stream stability at highway structures. Rep. No. FHWA-HI-96-032, FHWA, Washington D.C.1995. Pp. 56-59.
6. Okajima, A., Yi, D., Kimura, S., Kiwat, T. The blockage effects for an oscillating rectangular cylinder at moderate Reynolds number. Journal of Wind Engineering and Industrial Aerodynamics. 1997. Vol. 69–71. Pp. 997–1011.
7. Cigada, A., Malavasi, S., Vanali, M. Direct forces measurement on a submerged bridge model. Proceedings of the First International Conference on Fluid Structure Interaction. 26–28 September, Halkidiki, Greece. 2001. Pp. 305–314.
8. Malavasi, S., Guadagnini, A. Hydrodynamic loading on river bridges. J. Hydraul. Eng.. 2003. Vol. 129(11). Pp. 854–861.
9. Malavasi, S., Franzetti, S., Blois, G. PIV investigation of flow around submerged river bridge deck. River Flow 2004: Proc., 2ndInt. Conf. on Fluvial Hydraulics, Taylor and Francis, London, 2004. Pp. 601–608.
10. Malavasi, S., Guadagnini, A. Interactions between a rectangular cylinder and a free-surface flow. J. Fluids Struct. 2007. Vol. 23(8). Pp. 1137–1148.
11. Picek, T., Havlik, A., Mattas, D., Mares, K. Hydraulic calculation of bridges at high water stages. J. Hydraul. Res. 2007. No. 45(3). Pp. 400–406.
12. Malavasi, S., Trabucchi, N. Numerical investigation of the flow around a rectangular cylinder near a solid wall. Proc., Bluff Bodies Aerodynamics and Applications, Milano, Italy, 2008. Pp. 20–24.
13. Arslan, T., Malavasi, S., Pettersen, B., Andersson, H. Turbulent flow around a semi-submerged rectangular cylinder. J. Offshore Mech. Arct. Eng. 2013. Vol. 135(4). Pp. 0418011–04180111.
14. Chu Chia, Chih Jung Huang, Tso Ren Wu, Chung Yue Wang. Numerical simulation of hydrodynamic loading on submerged rectangular bridge decks. The Seventh International Colloquium on Bluff Body Aerodynamics and Applications (BBAA7), Shanghai, China, September 2–6, 2012. Pp. 1508–1517.
15. Chu Chia & Chung, Chun-Hsuan & Wu, Tso-Ren & Wang, Chung-Yue. Numerical Analysis of Free Surface Flow over a Submerged Rectangular Bridge Deck. Journal of Hydraulic Engineering. 2016. Vol. 143. Pp. 040160601–0401606011.
16. Hamill, L. Bridge hydraulics. E&FN Spon, London, 1999. 384 p.

17. Fox, R.W., McDonald, A.T., Pritchard, P.J. An introduction to fluid mechanics, 9th Ed., Wiley, New York, 2016. 672 p.
18. ANSYS Fluent Theory Guide. Release 15.0. ANSYS, Inc. November 2013. 814 p.
19. Shih, T.H., Liou, W.W., Shabbir, A., Yang, Z., Zhu, A New Eddy-Viscosity Model for High Reynolds Number Turbulent Flows – Model Development and Validation. Computers Fluids. 1995. Vol. 24(3). Pp. 227–238.
20. Launder, B.E.; Spalding, D.B. The numerical computation of turbulent flows. Computer Methods in Applied Mechanics and Engineering. 1974. Vol. 3(2). Pp. 269–289.
21. Hirt, C.W., Nichols, B.D. Volume of fluid (VOF) method for the dynamics of free boundaries. J. Comp. Phys. 1981. Vol. 39(1). Pp. 201–225.
22. Cigada, A., Malavasi, S., Vanali, M. Direct forces measurement on a submerged bridge model. Fluid structure interaction, WIT Press, Boston, 2001. Pp. 305–314.
23. Shimada, K., Ishihara, T. Application of a modified k−ε model to the prediction of aerodynamic characteristics of rectangular cross-section cylinders. J. Fluids Struct. 2002. Vol. 16(4). Pp. 465-485.
24. Lee, D., Nakagawa, H., Kawaike, K., Baba, Y., Zhang, H. Inundation flow considering overflow due to water level rise by river structures. Annuals of Disaster Prevention Research Institute, Kyoto University. 2010. No. 53 B. Pp. 607–616.
25. Ramamurthy, A.S., Junying, Qu, Oiep, Vo. Volume of fluid model for open channel flow problem. ǁ Canadian Journal of Civil Engineering. 2005. Vol. 32.5. Pp. 996–1001.
26. Zhaoding, X., Bushra, A., Anju, S.T, Kornel, K., Guo, J. CFD Modeling of drag and lift of inundated bridge decks. 33rd IAHR Congress held from August 10–14, 2009. Water Engineering for Sustainable Environment, Vancouver, Canada, 2009. Pp. 2575–2585.
27. Khrabry, A.I., Smirnov, E.M., Zaytsev, D.K. Numerical Study of wall friction effects on dambreak flows in the presence of an obstacle. 6th European Conference on Computational Fluid Dynamics (ECFD VI), 20–25 July 2014, Barcelona, Spain. Pp. 1–2.
28. Platonov, D.V., Minakov, A.V., Dekterev, A.A., Sentyabov, A.V. Chislennoye modelirovaniye prostranstvennykh techeniy s zakrutkoy potoka [Numerical modeling of spatial flows with spin flow]. Kompyuternyye issledovaniya i modelirovaniye. 2012. No. 2(1). Pp. 161–172. (rus)
29. Valger, S.A, Fedorov, A.V., Fedorova, N.N. Modelirovaniye neszhimayemykh turbulentnykh techeniy v okrestnosti plokhoobtekayemykh tel s ispolzovaniyem PK ANSYS [Fluent Simulation of incompressible turbulent flows in the vicinity of poorly streamlined bodies using the ANSIS Fluent PC]. Vychislitelnyye tekhnologii. 2013. No. 5(18). Pp. 27–40. (rus)
30. Khrabryy, A.I., Zaytsev, D.K., Smirnov, Ye.M. Chislennoye modelirovaniye techeniy so svobodnoy poverkhnostyu na osnove metoda VOF [Numerical simulation of free-surface flows based on the VOF method]. Trudy TsNII im. akad. A. N. Krylova (Trudy Krylovskogo gosudarstvennogo nauchnogo tsentra). 2013. Vyp. 78 (362). Pp. 53–64. (rus)
31. Khrabryy, A.I., Smirnov, Ye.M., Zaytsev, D.K. Vliyaniye modeli turbulentnosti na rezultaty rascheta obtekaniya prepyatstviya potokom vody posle obrusheniya damby [The influence of the turbulence model on the results of the calculation of the flow around an obstacle by the flow of water after the dam collapses]. Nauchno-tekhnicheskiye vedomosti SPbGPU. 2013. No. 1(165). Pp. 182–187. (rus)
32. Korkodinov, Ya.A. Obzor semeystva k-ε modeley dlya modelirovaniya turbulentnosti [An overview of the family of k-ε models for modeling turbulence]. Vestnik PNIPU. Mashinostroyeniye, materialovedeniye. 2013. No. 2(15). Pp. 5–16. (rus)

### *Contacts:*

*Thi Kim Chi Thai, +840988115110; chittk@utc.edu.vn*

Инженерно-строительный журнал

ISSN 2071-0305

сайт журнала: http://engstroy.spbstu.ru/

DOI: 10.18720/MCE.85.2

# Численное моделирование турбулентных потоков над подтопленными настилами мостов

***Т.К.Т. Тхай,***
*Университет транспорта и коммуникации, г. Ханой, Вьетнам*
*E-mail: chittk@utc.edu.vn*

**Ключевые слова:** настил моста; коэффициент сплошности конструкций; турбулентность; численное моделирование

**Аннотация.** В настоящее время изменение климата является одной из самых серьезных угроз и глобальных проблем. Оно вызывает увеличение числа стихийных бедствий, таких как ураганы, штормы, тайфуны и наводнения. В этих критических гидрологических условиях, транспортная инфраструктура, включающая в себя мосты, легко подтапливается, повреждается и разрушается. Оценка устойчивости моста, определение гидродинамических сил, действующих на мосты, и понимание сложного режима потока во время и после затопления, играют важную роль в определении вероятности возникновения рисков аварии для существующих мостов и оптимальной конструкции будущих мостов. В настоящей работе турбулентный поток с большим числом Рейнольдса над подтопленным настилом моста с различным соотношением длины к толщине был численно исследован с использованием программы ANSYS FLUENT. Соответственно, коэффициенты поджатия потока и затопления равны 0,23 и 2. Используемая $k$–$\varepsilon$ модель и объем фракции (VOF) были применены для прогнозирования совокупности профилей свободной поверхности воды над настилом моста и характеристики турбулентности, включая влияние подпора в верхнем бьефе моста. Была изучена зависимость соотношения длины к толщине настилов мостов от коэффициента сплошности конструкций.

## Литература

1. National disaster risk in Vietnam in the period 2006-2016 and forecasting and warning system. National Center for Hydro-Meteological Forecasting. Ministry of Natural Resources and Environment, Vietnam, 2017. 21 p.
2. The World Bank. Vietnam 2016: Rapid Flood Damage and Needs Assessment (RFDNA). 2016. 42 p.
3. NHMS: Statistics of annual major storms (Levels from 6 to 12) struck Vietnam between 1961 and 2014, National Hydro -Meteorological Service (NHMS), Ministry of Natural Resources and Environment, Vietnam, 2015.
4. Naudascher E., Medlarz H. J. Hydrodynamic loading and backwater effect of partially submerged bridges // J. Hydraul. Res. 1983. No. 21(3). Pp. 213–232.
5. Federal Highway Administration (FHWA). Stream stability at highway structures. Rep. No. FHWA-HI-96-032, FHWA, Washington D.C. 1995. Pp. 56–59.
6. Okajima A., Yi D., Kimura S., Kiwat T. The blockage effects for an oscillating rectangular cylinder at moderate Reynolds number // Journal of Wind Engineering and Industrial Aerodynamics. 1997. Vol. 69–71. Pp. 997–1011.
7. Cigada A., Malavasi S., Vanali M. Direct forces measurement on a submerged bridge model. Proceedings of the First International Conference on Fluid Structure Interaction. 26–28 September, Halkidiki, Greece. 2001. Pp. 305–314.
8. Malavasi S., Guadagnini A. Hydrodynamic loading on river bridges // J. Hydraul. Eng. 2003. Vol. 129 (11). Pp. 854–861
9. Malavasi S., Franzetti S., Blois G. PIV investigation of flow around submerged river bridge deck. River Flow 2004: Proc., 2ndInt. Conf. on Fluvial Hydraulics, Taylor and Francis, London, 2004. Pp. 601–608.
10. Malavasi S., Guadagnini A. Interactions between a rectangular cylinder and a free-surface flow // J. Fluids Struct. 2007. Vol. 23(8). Pp. 1137–1148.
11. Picek T., Havlik A., Mattas D., Mares K. Hydraulic calculation of bridges at high water stages // J. Hydraul. Res. 2007. No. 45(3). Pp. 400–406.
12. Malavasi S., Trabucchi N. Numerical investigation of the flow around a rectangular cylinder near a solid wall // Proc., Bluff Bodies Aerodynamics and Applications, Milano, Italy, 2008. Pp. 20–24.
13. Arslan T., Malavasi S., Pettersen B., Andersson H. Turbulent flow around a semi-submerged rectangular cylinder // J. Offshore Mech. Arct. Eng. 2013. Vol. 135(4). Pp. 0418011–04180111.
14. Chu Chia, Chih Jung Huang, Tso Ren Wu, Chung Yue Wang. Numerical simulation of hydrodynamic loading on submerged rectangular bridge decks. The Seventh International Colloquium on Bluff Body Aerodynamics and Applications (BBAA7), Shanghai, China, September 2–6, 2012. Pp. 1508–1517.

15. Chu Chia & Chung, Chun-Hsuan & Wu, Tso-Ren & Wang, Chung-Yue. Numerical Analysis of Free Surface Flow over a Submerged Rectangular Bridge Deck // Journal of Hydraulic Engineering. 2016. Vol. 143. Pp. 040160601–0401606011.
16. Hamill L. Bridge hydraulics. E&FN Spon, London, 1999. 384 p.
17. Fox R.W., McDonald A.T., Pritchard P.J. An introduction to fluid mechanics, 9th Ed., Wiley, New York, 2016. 672 p.
18. ANSYS Fluent Theory Guide. Release 15.0. ANSYS, Inc. November 2013. 814 p.
19. Shih T.H., Liou W.W., Shabbir A., Yang Z., Zhu. A New Eddy-Viscosity Model for High Reynolds Number Turbulent Flows – Model Development and Validation. Computers Fluids. 1995. Vol. 24(3). Pp. 227–238.
20. Launder B.E.; Spalding D.B. The numerical computation of turbulent flows // Computer Methods in Applied Mechanics and Engineering. 1974. Vol. 3(2). Pp. 269–289.
21. Hirt C.W., Nichols B.D. Volume of fluid (VOF) method for the dynamics of free boundaries // J. Comp. Phys. 1981. Vol. 39(1). Pp. 201–225.
22. Cigada A., Malavasi S., Vanali M. Direct forces measurement on a submerged bridge model. Fluid structure interaction, WIT Press, Boston, 2001. Pp. 305–314.
23. Shimada K., Ishihara T. Application of a modified k−ε model to the prediction of aerodynamic characteristics of rectangular cross-section cylinders // J. Fluids Struct. 2002. Vol. 16(4), Pp. 465–485.
24. Lee D., Nakagawa H., Kawaike K., Baba Y., Zhang H. Inundation flow considering overflow due to water level rise by river structures // Annuals of Disaster Prevention Research Institute, Kyoto University. 2010. No. 53 B. Pp. 607–616.
25. Ramamurthy A.S., Junying Qu, Oiep Vo. Volume of fluid model for open channel flow problem // ‖ Canadian Journal of Civil Engineering. 2005. Vol. 32.5. Pp. 996–1001.
26. Zhaoding X., Bushra A., Anju S.T, Kornel K., Guo J. CFD Modeling of drag and lift of inundated bridge decks // 33rd IAHR Congress held from August 10–14, 2009. Water Engineering for Sustainable Environment, Vancouver, Canada, 2009. Pp. 2575–2585.
27. Khrabry A.I., Smirnov E.M., Zaytsev D.K. Numerical Study of wall friction effects on dambreak flows in the presence of an obstacle // 6th European Conference on Computational Fluid Dynamics (ECFD VI), 20–25 July 2014, Barcelona, Spain. Pp. 1–2.
28. Платонов Д.В. , Минаков А.В., Дектерев А.А., Сентябов А.В. Численное моделирование пространственных течений с закруткой потока // Компьютерные исследования и моделирование. 2012. № 2(1). С. 161–172.
29. Вальгер С.А, Федоров А.В., Федорова Н.Н. Моделирование несжимаемых турбулентных течений в окрестности плохообтекаемых тел с использованием ПК ANSYS Fluent // Вычислительные технологии. 2013. № 5(18). С. 27–40.
30. Храбрый А.И., Зайцев Д.К., Смирнов Е.М. Численное моделирование течений со свободной поверхностью на основе метода VOF // Труды ЦНИИ им. акад. А.Н. Крылова (Труды Крыловского государственного научного центра). 2013. Вып. 78 (362). С. 53–64.
31. Храбрый А.И., Смирнов Е.М., Зайцев Д.К. Влияние модели турбулентности на результаты расчета обтекания препятствия потоком воды после обрушения дамбы // Научно-технические ведомости СПбГПУ. 2013. № 1 (165). С. 182–187.
32. Коркодинов Я.А. Обзор семейства k-ε моделей для моделирования турбулентности // Вестник ПНИПУ. Машиностроение, материаловедение. 2013. № 2(15). С. 5–16.

### *Контактные данные:*

*Тхи Ким Тьи Тхай, +840988115110; эл. почта: chittk@utc.edu.vn*